

Hadron spectra, flow and correlations in PbPb collisions at the LHC: interplay between soft and hard physics

I.P. Lokhtin¹, A.V. Belyaev¹, L.V. Malinina^{1,2}, S.V. Petrushanko¹, E.P. Rogochaya² and A.M. Snigirev¹

¹ Skobeltsyn Institute of Nuclear Physics, Lomonosov Moscow State University, Moscow, Russia

² Joint Institute for Nuclear Research, Dubna, Russia

Abstract. The started LHC heavy ion program makes it possible to probe new frontiers of the high temperature Quantum Chromodynamics. It is expected that the role of hard and semi-hard particle production processes may be significant at ultra-high energies even for bulk properties of the created matter. In this paper, the LHC data on multiplicity, hadron spectra, elliptic flow and femtoscopic correlations from PbPb collisions at center-of-mass energy 2.76 TeV per nucleon pair are analyzed in the framework of the HYDJET++ model. The influence of the jet production mechanism on these observables is discussed.

1 Introduction

One of the main aims of modern high energy physics is to study the strong interaction in extreme regimes at super-high densities and temperatures. Hot and dense multi-parton and multi-hadron systems are produced in high-energy nuclear collisions and can be investigated within the Quantum Chromodynamics (QCD) (see, e.g., recent reviews [1,2,3,4]). The experimental and phenomenological study of multi-particle production in ultrarelativistic heavy ion collisions is expected to provide valuable information on the dynamical behavior of QCD matter in the form of the quark-gluon matter (QGM), as predicted by lattice calculations. The current lead-lead (PbPb) collision center-of-mass energy per nucleon pair at LHC, $\sqrt{s_{NN}} = 2.76$ TeV, is a factor of ~ 14 larger than that at RHIC and makes it possible to probe new frontiers of the super-high temperature and (almost) net-baryon free QCD. It is expected that a role of hard and semi-hard particle production may be significant at ultra-high energies even for bulk properties of the created matter.

A number of striking LHC results from PbPb runs have been published by ALICE [5,6,7,8,9,10,11,12,13,14,15,16,17], ATLAS [18,19,20,21,22] and CMS [23,24,25,26,27,28,29,30,31,32,33,34,35,36] collaborations (see [37] for the overview of the results from the first year of heavy ion physics at LHC). In the paper, we analyze the LHC data on multiplicity, hadron spectra, elliptic flow and femtoscopic momentum correlations from PbPb collisions at $\sqrt{s_{NN}} = 2.76$ TeV in the framework of the HYDJET++ model [38]. The main goal of this study is to show a significant influence of the (in-medium) jet production mechanism on the global event pattern at LHC. Note that the influence of the interactions between jets and soft hadrons on a number of physical observables at the LHC was studied recently in the framework of the EPOS model [39].

2 HYDJET++ model

HYDJET++ (the successor of HYDJET [40]) is the model of relativistic heavy ion collisions, which includes two independent components: the soft state (hydro-type) and the hard state resulting from the in-medium multi-parton fragmentation. The details of the used physics model and simulation procedure can be found in the HYDJET++ manual [38]. Below main features of the model are described only very briefly.

2.1 Soft component

The soft component of an event in HYDJET++ is the “thermal” hadronic state generated on the chemical and thermal freeze-out hypersurfaces obtained from the parametrization of relativistic hydrodynamics with preset freeze-out conditions (the adapted event generator FAST MC [41,42]). Hadron multiplicities are calculated using the effective thermal volume approximation and Poisson multiplicity distribution around its mean value, which is supposed to be proportional to a number of participating nucleons for a given impact parameter of a AA collision. To simulate the elliptic flow effect, the hydro-inspired parametrization is implemented for the momentum and spatial anisotropy of a soft hadron emission source [38,43].

The soft hadron simulation procedure includes the following steps.

- Generation of a hadron 4-momentum in the liquid element rest frame in accordance with the equilibrium distribution function.
- Generation of a spatial position and local 4-velocity of the liquid element in accordance with the phase space and the character of fluid motion.

- Standard von Neumann rejection/acceptance procedure to account for a difference between the true and generated probabilities.
- Boost of the hadron 4-momentum in the event center-of-mass frame.
- Taking into account two- and three-body decays of resonances with branching ratios taken from the SHARE particle decay table [44].

The model has a number of input parameters for the soft component. They are tuned from fitting to experimental data values for various physical observables (see the next section). Parameters which determine the hadron ratios are the chemical freeze-out temperature T_{ch} and thermodynamical potentials (baryon potential μ_{B} , strangeness potential μ_{S} , isospin potential μ_{Q} , and potential of positively charged pions μ_{π}^{th} at thermal freeze-out). We have used $T_{\text{ch}} = 165$ MeV and, for simplicity, zero thermodynamical potentials. The collective flow parameters are the maximal longitudinal and transverse flow rapidities, $Y_{\text{L}}^{\text{max}} = 4.5$ and $Y_{\text{T}}^{\text{max}} = 1.265$, respectively. The latter value has been fixed from the data on hadron p_{T} -spectra together with the thermal freeze-out temperature $T_{\text{th}} = 105$ MeV. The total multiplicity of the soft component is determined by space-time parameters on the thermal freeze-out for central collisions, maximal transverse radius $R_{\text{f}}(b = 0)$, proper time $\tau_{\text{f}}(b = 0)$ and the duration of hadron emission $\Delta\tau_{\text{f}}(b = 0)$. These parameters have been fixed from fitting of three-dimensional correlation functions measured for $\pi^+\pi^+$ pairs and extracting the correlation radii: $R_{\text{f}}(b = 0) = 13.45$ fm, $\tau_{\text{f}}(b = 0) = 12.2$ fm/c, $\Delta\tau_{\text{f}}(b = 0) = 2$ fm/c.

2.2 Hard component

The model used for the hard component in HYDJET++ is the same as in the HYDJET event generator. It is based on the PYQUEN partonic energy loss model [40]. The approach describing the multiple scattering of hard partons is based on accumulated energy loss via gluon radiation which is associated with each parton scattering in expanding quark-gluon fluid. It also includes the interference effect in gluon emission with a finite formation time using the modified radiation spectrum dE/dx as a function of the decreasing temperature T . The model takes into account radiative and collisional energy loss of hard partons in longitudinally expanding quark-gluon fluid, as well as the realistic nuclear geometry. Radiative energy loss is treated in the framework of the BDMS model [45,46] with a simple generalization to a massive quark case using the “dead-cone” approximation [47]. The collisional energy loss due to elastic scatterings is calculated in the high-momentum transfer limit [48,49,50]. The strength of the energy loss in PYQUEN is determined mainly by the initial maximal temperature T_0^{max} of hot matter in central PbPb collisions (i.e. an initial temperature in the center of the nuclear overlap at mid-rapidity). The energy loss depends also on the proper time τ_0 of QGM formation and the number N_{f} of active flavors

in the medium. The parameter values $T_0^{\text{max}} = 1$ GeV, $\tau_0 = 0.1$ fm/c and $N_{\text{f}} = 0$ (gluon-dominated plasma) are used at $\sqrt{s_{\text{NN}}} = 2.76$ TeV. Another important ingredient of PYQUEN is the angular spectrum of in-medium radiation. Since the ATLAS [18] and CMS [23] data on the dijet asymmetry support the supposition of the “out-of-cone” medium-induced partonic energy loss, the “wide-angular” parametrization of medium-induced gluon radiation [51] is used in the presented investigation.

The simulation of single hard nucleon-nucleon sub-collisions by PYQUEN is constructed as a modification of the jet event obtained with the generator of hadron-hadron interactions PYTHIA_6.4 [52]. We used PYTHIA tune Pro-Q20 for the present simulation. It reproduces the CMS data on hadron momentum spectra in pp collisions at LHC energies with the 10–15% accuracy in the full measured p_{T} -range [53].

The event-by-event simulation procedure in PYQUEN includes the following steps.

- Generation of initial parton spectra with PYTHIA and production vertices at a given impact parameter.
- Rescattering-by-rescattering simulation of the parton path in a dense zone and its radiative and collisional energy loss.
- Final hadronization according to Lund string model for hard partons and in-medium emitted gluons.

Then the number of PYQUEN jets is generated according to the binomial distribution. The mean number of jets produced in an AA event is calculated as a product of the number of binary NN sub-collisions at a given impact parameter per the integral cross section of the hard process in NN collisions with the minimum transverse momentum transfer $p_{\text{T}}^{\text{min}}$. The latter is an input parameter of the model. In the framework of HYDJET, partons produced in (semi)hard processes with the momentum transfer lower than $p_{\text{T}}^{\text{min}}$, are considered as being “thermalized”. So, their hadronization products are included “automatically” in the soft component of the event. In order to take into account the effect of nuclear shadowing on parton distribution functions, we use the impact parameter dependent parametrization obtained in the framework of Glauber-Gribov theory [54]. The nuclear shadowing correction factor $S(r_1, r_2, x_1, x_2, Q^2)$ depends on kinematic variables of incoming hard partons (the momentum fractions $x_{1,2}$ of initial partons from incoming nuclei and the momentum scale Q^2 of a hard scattering), and on the transverse coordinates $r_{1,2}$ of partons in their parent nuclei. This initial state effect reduces the number of partons in the incoming hadronic wave-functions of both nuclei and, thus, reduces the yield of high- p_{T} hadrons coming from jets (in addition to the medium-induced partonic energy loss).

To study the femtoscopic (HBT) momentum correlations, it is necessary to specify a space-time structure of a hadron emission source. The information about final particle 4-momenta and 4-coordinates of emission points is automatically recorded using the soft hadron simulation procedure (see previous subsection). For the hard component, the existence of a “source” with a given size is not obvious and is a matter of discussion (see, for instance,

[55]). The point of jet hadronization and the point of initial parton-parton hard scattering do not coincide. In accordance with [55], we assume that hadronization occurs at different distances from an initial hard scattering, depending on an energy of a jet.

Our treatment of the coordinate information for low momentum jet particles with $p_T < 1$ GeV/ c is similar to one for directly produced hadrons from soft component. Such particles are emitted from the fireball of radius R_f at mean proper time τ_f with the emission duration $\Delta\tau_f$.

Four-coordinates of high momentum jet particles with $p_T > 1$ GeV/ c are shifted from those of a jet vertex and coded in the following way [55]:

$$\begin{aligned} x_i &= x_0 + L_{li} \frac{\cos \phi_j}{\cosh y_j} + L_{t1i} \frac{\cos \phi_j \sinh y_j}{\cosh y_j} - L_{t2i} \sin \phi_j \\ y_i &= y_0 + L_{li} \frac{\sin \phi_j}{\cosh y_j} + L_{t1i} \frac{\sin \phi_j \sinh y_j}{\cosh y_j} + L_{t2i} \cos \phi_j \\ z_i &= z_0 + L_{li} \frac{\sinh y_j}{\cosh y_j} - L_{t1i} \frac{1}{\cosh y_j} \\ t_i &= t_0 + L_{li}, \end{aligned} \quad (1)$$

where the subscripts i and j refer to particles and jets respectively. Here $x_0 = r \cos \psi$ and $y_0 = r \sin \psi$ are transverse coordinates of a jet production vertex, r is a distance from the nuclear collision axis to the vertex with the azimuthal angle ψ . The longitudinal position and the initial time of a hard process are estimated as $z_0 \simeq \sinh y_j / p_{Tj}$ and $t_0 \simeq \cosh y_j / p_{Tj}$, respectively (ϕ_j and y_j are the azimuthal angle and the pseudorapidity of a jet, respectively). For each hadron i , the localization L_{li} of hadronization along the direction of a jet is randomized from Gaussian distributions with mean l_i and variance $\sigma = l_i/3$ [55]. The hadronization points L_{t1i} and L_{t2i} (with respect to the jet direction) are randomized in the transverse direction from a Gaussian distribution with variance $\sigma_t = 0.5$ fm and zero mean value; l_i is assumed to be proportional to jet momentum $|\mathbf{p}_j|$. Thus, $l_i = f|\mathbf{p}_j|$ where f is a multiplicative factor that represents our lack of theoretical insight into the process of hadronization (the value $f = 5$ being used in our simulations). For simplicity, the jet axis is determined by the momentum direction of a leading particle in the event. Then four-coordinates of jet particles with $p_T > 1$ GeV/ c are shifted from the jet vertex position along or opposite this direction depending on a sign of the scalar production ($\mathbf{p}_i \mathbf{p}_j$).

3 Numerical results and discussion

It was demonstrated in [38] that the HYDJET++ model can describe bulk properties of the hadronic state created in AuAu collisions at RHIC at $\sqrt{s_{NN}} = 200$ GeV (hadron spectra and ratios, radial and elliptic flow, femtoscopic momentum correlations), as well as the high- p_T hadron spectra. At present we apply HYDJET++ with tuned input parameters to reproduce the LHC data from PbPb collisions, and to estimate an influence of the hard production mechanism on physics observables.

3.1 Centrality and pseudorapidity dependence of multiplicity

Figure 1 shows the charged multiplicity density at mid-rapidity (normalized on the mean number of participating nucleons $\langle N_{\text{part}} \rangle$) as a function of event centrality (left) and pseudorapidity distribution in two centrality bins (right) in PbPb collisions at $\sqrt{s_{NN}} = 2.76$ TeV. The results of HYDJET++ simulation are compared with the ALICE [7] and CMS [27] data. Since multiplicities from soft and hard components depend on the centrality in a different way, the relative contribution of soft and hard components to the total event multiplicity can be fixed through the centrality dependence of $dN/d\eta$. The latter can be reproduced at $\sim 25\%$ contribution of the hard component (versus $\sim 15\%$ at RHIC [38]) in most central collisions, and it decreases for more peripheral events. This contribution of the hard component corresponds to the minimal transverse momentum transfer of parton-parton scatterings $p_T^{\text{min}} = 8.2$ GeV/ c . The approximately flat η dependence of the multiplicity observed by CMS (the variation being less than 10% in the pseudorapidity range $|\eta| < 2.5$) is also well reproduced by HYDJET++ simulation for different event centralities at reasonable values of maximal longitudinal flow rapidity, $Y_L^{\text{max}} = 3.5 \div 4.5$.

The ratios of mid-rapidity yields of final charged hadrons in the model (excluding weak decays of strange hadrons) are $K^\pm/\pi^\pm = 0.153$ and $p^\pm/\pi^\pm = 0.065$ at 0–5% of PbPb centrality. The calculated kaon-to-pion ratio reproduces the experimental number reported by ALICE [56] (0.155 ± 0.012), while the proton-to-pion ratio is overestimated in the model by $\sim 40\%$ as compared with the ALICE data (0.046 ± 0.004). Since pure thermal models meet with difficulties to reproduce these hadron ratios, in our opinion, it may be interpreted as a significant influence of (mini-)jet production on a particle composition in heavy ion collisions (hadron ratios for soft and hard components are quite different).

3.2 Transverse momentum spectrum and nuclear modification factor

Figure 2 (left) shows the transverse momentum spectrum of charged particles ($|\eta| < 0.8$) in 5% of most central PbPb collisions at $\sqrt{s_{NN}} = 2.76$ TeV. The results of HYDJET++ simulation are compared with the ALICE data [8]. The slope of p_T -spectra allows one to fix the thermal freeze-out temperature $T^{\text{th}} = 105$ MeV and the maximal transverse flow rapidity $Y_T^{\text{max}} = 1.265$. One can see that HYDJET++ reproduces the measured p_T -spectrum for central PbPb events at least up to eight orders of cross section magnitude. Multiplicities of the hard and soft components become comparable at $p_T \sim 4.5$ GeV/ c .

High transverse momentum region of hadron spectra ($p_T > 5 \div 10$ GeV/ c) is sensitive to parton production and jet quenching. In HYDJET++, they are determined by the PYQUEN parameters for initial conditions of QGM formation [51]. The nuclear modification factor R_{AA} is defined as a ratio of particle yields in AA and pp collisions

normalized on the mean number of binary nucleon-nucleon sub-collisions $\langle N_{\text{coll}} \rangle$:

$$R_{AA}(p_T) = \frac{d^2 N^{AA}/d\eta dp_T}{\langle N_{\text{coll}} \rangle d^2 N^{PP}/d\eta dp_T}. \quad (2)$$

In the absence of nuclear effects (in initial or final states) at high p_T , it should be $R_{AA} = 1$. In figure 2 (right), the calculated nuclear modification factor $R_{AA}(p_T)$ for charged hadrons ($|\eta| < 1$) is compared with the CMS data [29] in 5% of most central PbPb collisions. The reasonable agreement with the data is achieved up to $p_T \sim 100$ GeV/ c . However the simulated p_T -dependence of R_{AA} looks rather weaker than the tendency of the data. It could indicate that the real energy dependence of partonic energy loss is somewhat weaker than it is expected from the model simulations. It is worth to remind here that the energy dependence of BDMS radiative loss [45,46] (the dominant mechanism of medium-induced energy loss in PYQUEN) is between $\Delta E \propto \ln E$ and $\Delta E \propto \sqrt{E}$ (depending on the energy of the radiated gluon and on the properties of the medium).

3.3 Femtoscopic momentum correlations

Effects of quantum statistics and final state interactions make the momentum (HBT) correlation functions of two or more particles in their c.m.s. sensitive to space-time characteristics of production process on the level of femtometers at small relative momenta. Since HYDJET++ specifies the space-time structure of a hadron emission source (for both soft and hard components), the momentum correlation function can be introduced by the standard weighting procedure [57,58]. Having the information about final particle 4-momenta p_i and 4-coordinates x_i of emission points, we can calculate the correlation function with the help of the weight procedure, assigning a weight to a given particle combination and accounting for effects of quantum statistics:

$$w = 1 + \cos(q \cdot \Delta x), \quad (3)$$

where $q = p_1 - p_2$ and $\Delta x = x_1 - x_2$. Then the correlation function is defined as a ratio of a weighted histogram of pair kinematic variables to an unweighted one. The corresponding correlation widths are parametrized in terms of the Gaussian correlation radii R_i as follows:

$$CF(p_1, p_2) = 1 + \lambda \exp(-R_{\text{out}}^2 q_{\text{out}}^2 - R_{\text{side}}^2 q_{\text{side}}^2 - R_{\text{long}}^2 q_{\text{long}}^2), \quad (4)$$

where $\mathbf{q} = (q_{\text{out}}, q_{\text{side}}, q_{\text{long}})$ is the relative three-momentum vector of two identical particles and λ is the correlation strength. The “out” axis is pointing along the pair transverse momentum, the “side” axis is perpendicular to the “out” direction in the transverse plane, and the “long” axis is along the beam.

Figure 3 shows the fitted correlation radii as a function of mean transverse momentum k_T of pion pair ($|\eta| < 0.8$)

in 5% of most central PbPb collisions at $\sqrt{s_{\text{NN}}} = 2.76$ TeV. The results of the HYDJET++ simulation are compared with the ALICE data [9]. Taking into account both soft and hard components allows us to reproduce the measured k_T -dependencies of the correlation radii.

Let us comment how our relatively simple model without detailed fluid dynamic evolution and hadronic cascade is able to fit the experimental data on the femtoscopic observables. In fact, there are 3D-hydrodynamics models which reproduce HBT radius parameters in heavy ion collisions at RHIC and LHC energies, e.g. [59,60]. A successful simultaneous description of hadronic yields and spectra, elliptic flow and correlation radii at RHIC and LHC is achieved also in hydro-kinetic model [61]. These approaches include the hydrodynamical evolution and hadronic cascade calculations which are very computer time consuming. HYDJET++ is the multi-purpose event generator for a fast simulation (needed e.g. in Monte-Carlo studies of the experimental setup), and so it does not contain detailed hydrodynamical evolution and hadronic cascade. The treatment of the soft component in HYDJET++ is based on the fast simulation of the freeze-out hypersurface realized in FAST MC model [41,42] describing well the femtoscopic radii at RHIC energies. The main feature of this approach is that the hadron system expands hydrodynamically with the frozen chemical composition, cools down, and finally decays at some thermal freeze-out hypersurface. The chemical potentials are fixed from the experimental particle number ratios at the chemical freeze-out. In spite of lack of the hydrodynamical evolution in HYDJET++, the assumption of the conservation of the particle number ratios from the chemical to thermal freeze-out allows us to calculate the chemical potentials at the thermal freeze-out. The absolute values of particle densities are determined by the free parameter of the model, effective pion chemical potential μ_{π}^{th} at the thermal freeze-out. The best tune of the temperatures at chemical and thermal freeze-out hypersurfaces and volume parameters allow us to reproduce simultaneously the data on the total multiplicity, hadronic spectra and correlation radii. At the same time, low momentum particles (with $p_T < 1$ GeV/ c) coming from the hard component are emitted from the same thermal freeze-out hypersurface as soft component hadrons (see subsection 2.2).

3.4 Elliptic flow

The elliptic flow coefficient v_2 is defined as the second-order Fourier coefficient in the hadron distribution over the azimuthal angle φ relative to the reaction plane angle ψ_R , so that $v_2 \equiv \langle \cos 2(\varphi - \psi_R) \rangle$. It is an important characteristic of physics dynamics at early stages of non-central heavy ion collisions. According to the typical hydrodynamic scenario, values of $v_2(p_T)$ at low- p_T are determined mainly by internal pressure gradients of an expanding fireball during the initial high density phase of the reaction, while the elliptic flow at high- p_T is generated due to partonic energy loss in an azimuthally asymmetric

volume of QGM. Figures 4 and 5 show elliptic flow coefficient v_2 as a function of the hadron transverse momentum p_T and pseudorapidity η , respectively. The results of the HYDJET++ simulation are compared with the CMS data obtained from the 4-particle cumulant method [33]. HYDJET++ reproduces η -dependence and p_T dependence of v_2 at mid-rapidity (up to $p_T \sim 5$ GeV/ c and 40% centrality). As it is expected, taking into account the hard component changes the hydrodynamical growth of v_2 with p_T , so v_2 decreases at $p_T > 3 \div 4$ GeV/ c . The flat η -dependence of v_2 manifests the strong longitudinal flow effect taken into account in HYDJET++.

4 Conclusions

The LHC data on multiplicity, hadron spectra, elliptic flow and femtoscopic momentum correlations in PbPb collisions at $\sqrt{s_{NN}} = 2.76$ TeV are analyzed in the framework of the HYDJET++ model. The significant influence of the jet production mechanism on these observables is shown. We have estimated that the contribution of the hard component to the total multiplicity is about 25% at mid-rapidity in most central collisions, and it decreases for more peripheral events.

Taking into account both hard and soft components and tuning input parameters allow HYDJET++ to reproduce the LHC data on centrality and pseudorapidity dependence of charged particle multiplicity, p_T -spectra, nuclear modification factor (up to $p_T \sim 100$ GeV/ c) and $\pi^\pm\pi^\pm$ correlation radii in central PbPb collisions, and p_T - and η -dependencies of the elliptic flow coefficient v_2 (up to $p_T \sim 5$ GeV/ c and 40% centrality).

Discussions with I. Arsene, L. Bravina, D. d'Enterria, A. Griubshin, V. Korotkikh, L. Sarycheva, Yu. Sinyukov, K. Tiwonyuk and E. Zabrodin are gratefully acknowledged. We thank colleagues from CMS and ALICE collaborations for fruitful cooperation. This work was supported by Russian Foundation for Basic Research (grants 10-02-93118 and 12-02-91505), Grant of President of Russian Federation for scientific Schools supporting (3920.2012.2) and Dynasty Foundation.

References

1. D. d'Enterria, J. Phys. **G 34**, (2007) S53
2. P. Braun-Munzinger and J. Stachel, Nature **448**, (2007) 302
3. C. Salgado, Proceedings of European School of High-Energy Physics (2008) 239, arXiv:0907.1219 [hep-ph]
4. I.M. Dremin, A.V. Leonidov, Phys. Usp. **53**, (2011) 1123
5. K. Aamodt, et al. (ALICE Collaboration), Phys. Rev. Lett. **105**, (2010) 252301
6. K. Aamodt, et al. (ALICE Collaboration), Phys. Rev. Lett. **105**, (2010) 252302
7. K. Aamodt, et al. (ALICE Collaboration), Phys. Lett. **B 696**, (2011) 30
8. K. Aamodt, et al. (ALICE Collaboration), Phys. Rev. Lett. **106**, (2011) 032301
9. K. Aamodt, et al. (ALICE Collaboration), Phys. Lett. **B 696**, (2011) 328
10. K. Aamodt, et al. (ALICE Collaboration), Phys. Rev. Lett. **107**, (2011) 032301
11. K. Aamodt, et al. (ALICE Collaboration), Phys. Lett. **B 708**, (2012) 249
12. K. Aamodt, et al. (ALICE Collaboration), Phys. Rev. Lett. **108**, (2012) 092301
13. B. Abelev, et al. (ALICE Collaboration), JHEP **1203**, (2012) 053
14. B. Abelev, et al. (ALICE Collaboration), arXiv:1202.1383 [hep-ex]
15. B. Abelev, et al. (ALICE Collaboration), arXiv:1203.2160 [nucl-ex]
16. B. Abelev, et al. (ALICE Collaboration), arXiv:1203.2436 [nucl-ex]
17. B. Abelev, et al. (ALICE Collaboration), arXiv:1205.5761 [nucl-ex]
18. G. Aad, et al. (ATLAS Collaboration), Phys. Rev. Lett. **105**, (2010) 252303
19. G. Aad, et al. (ATLAS Collaboration), Phys. Lett. **B 697**, (2011) 294
20. G. Aad, et al. (ATLAS Collaboration), Phys. Lett. **B 707**, (2012) 330
21. G. Aad, et al. (ATLAS Collaboration), Phys. Lett. **B 710**, (2012) 363
22. G. Aad, et al. (ATLAS Collaboration), arXiv:1203.3087 [hep-ex]
23. S. Chatrchyan, et al. (CMS Collaboration), Phys. Rev. **C 84**, (2011) 024906
24. S. Chatrchyan, et al. (CMS Collaboration), Phys. Rev. Lett. **106**, (2011) 212301
25. S. Chatrchyan, et al. (CMS Collaboration), JHEP **1107**, (2011) 076
26. S. Chatrchyan, et al. (CMS Collaboration), Phys. Rev. Lett. **107**, (2011) 052302
27. S. Chatrchyan, et al. (CMS Collaboration), JHEP **1108**, (2011) 141
28. S. Chatrchyan, et al. (CMS Collaboration), Phys. Lett. **B 710**, (2012) 256
29. S. Chatrchyan, et al. (CMS Collaboration), Eur. Phys. J. **C 72**, (2012) 1945
30. S. Chatrchyan, et al. (CMS Collaboration), JHEP **1205**, (2012) 063
31. S. Chatrchyan, et al. (CMS Collaboration), Phys. Lett. **B 712**, (2012) 176
32. S. Chatrchyan, et al. (CMS Collaboration), arXiv:1201.3158 [nucl-ex]
33. S. Chatrchyan, et al. (CMS Collaboration), arXiv:1204.1409 [nucl-ex]
34. S. Chatrchyan, et al. (CMS Collaboration), arXiv:1204.1850 [nucl-ex]
35. S. Chatrchyan, et al. (CMS Collaboration), arXiv:1205.0206 [nucl-ex]
36. S. Chatrchyan, et al. (CMS Collaboration), arXiv:1205.2488 [nucl-ex]
37. B. Muller, J. Schukraft, B. Wyslouch, arXiv:1202.3233 [hep-ex]
38. I.P. Lokhtin, L.V. Malinina, S.V. Petrushanko, A.M. Snigirev, I. Arsene, K. Tywoniuk, Comput. Phys. Commun. **180**, (2009) 779
39. K. Werner, Iu. Karpenko, M. Bleicher, T. Pierog, S. Porteboeuf-Houssais, arXiv:1203.5704 [nucl-th]

40. I.P. Lokhtin, A.M. Snigirev, Eur. Phys. J. **C 45**, (2006) 211
41. N.S. Amelin et al., Phys. Rev. **C 74**, (2006) 064901
42. N.S. Amelin et al., Phys. Rev. **C 77**, (2008) 014903
43. U. Wiedemann, Phys. Rev. **C 57**, (1998) 266
44. G. Torrieri, S. Steinke, W. Broniowski, W. Florkowski, J. Letessier, J. Rafelski, Comput. Phys. Commun. **167**, (2005) 229
45. R. Baier, Yu. L. Dokshitzer, A.H. Mueller, D. Schiff, Phys. Rev. **C 60**, (1999) 064902
46. R. Baier, Yu. L. Dokshitzer, A.H. Mueller, D. Schiff, Phys. Rev. **C 64**, (2001) 057902
47. Yu.L. Dokshitzer, D. Kharzeev, Phys. Lett. **B 519**, (2001) 199
48. J.D. Bjorken, Fermilab publication Pub-82/29-THY, 1982
49. E. Braaten, M. Thoma, Phys. Rev. **D 44**, (1991) 1298
50. I.P. Lokhtin, A.M. Snigirev, Eur. Phys. J. **C 16**, (2000) 527
51. I.P. Lokhtin, A.V. Belyaev, A.M. Snigirev, Eur. Phys. J. **C 71**, (2011) 1650
52. T. Sjostrand, S. Mrenna, P. Skands, JHEP **0605**, (2006) 026
53. S. Chatrchyan, et al. (CMS Collaboration), JHEP **1108**, (2011) 086
54. K. Tywoniuk, I.C. Arsene, L. Bravina, A.B. Kaidalov, E. Zabrodin, Phys. Lett. **B 657**, (2007) 170
55. G. Paic, P.K. Skowronski, J.Phys. **G 31**, (2005) 1045
56. M. Floris (for the ALICE Collaboration), J. Phys. **G 38**, (2011) 124025
57. M.I. Podgoretsky, Sov. J. Nucl. Phys. **37**, (1983) 272
58. S. Pratt, Phys. Rev. Lett. **53**, (1984) 1219
59. Yu. Karpenko, Yu. Sinyukov, Phys.Lett. **B 688**, (2010) 50
60. P. Bozek, Phys. Rev. **C 85**, (2012) 034901
61. I.A. Karpenko, Y.M. Sinyukov, K. Werner, arXiv:1204.5351 [nucl-th]

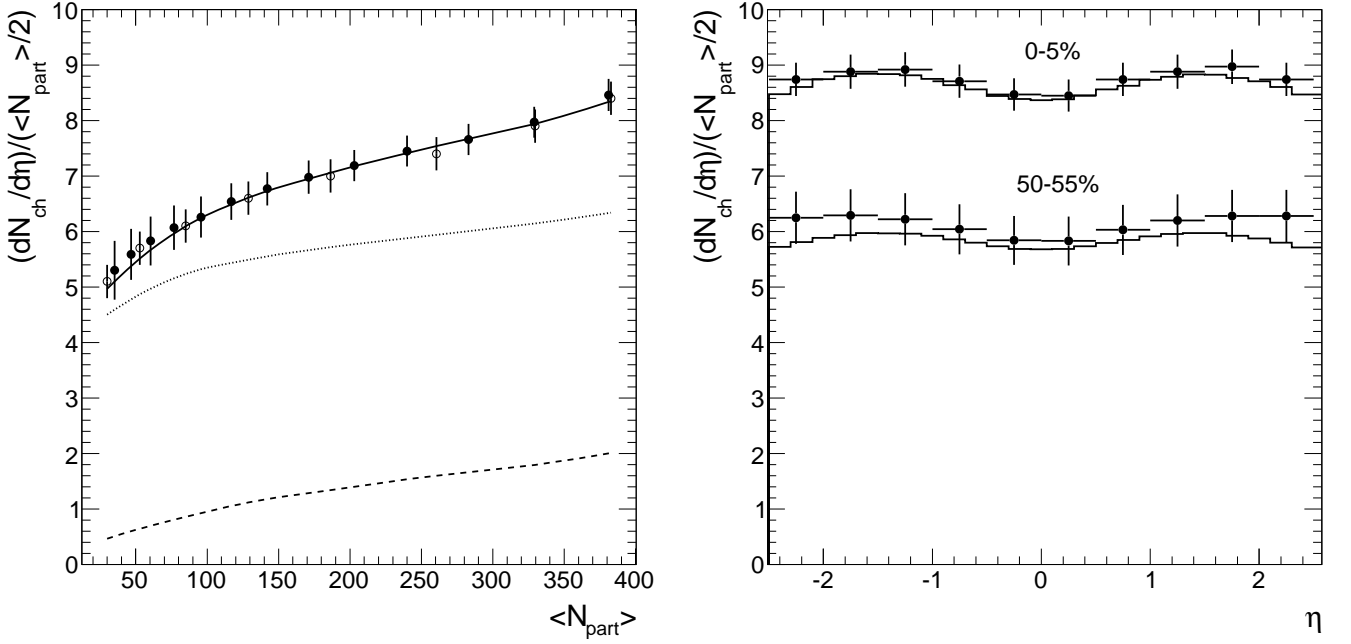


Fig. 1. Charged multiplicity density at mid-rapidity (normalized on the mean number of participating nucleons $\langle N_{part} \rangle$) as a function of PbPb event centrality (left) and pseudorapidity distribution in two centrality bins (right) at $\sqrt{s_{NN}} = 2.76$ TeV. The open and closed points are ALICE [7] and CMS [27] data respectively, curves (left) and histograms (right) are the simulated HYDJET++ events (solid – total result, dashed – hard component, dotted – soft component).

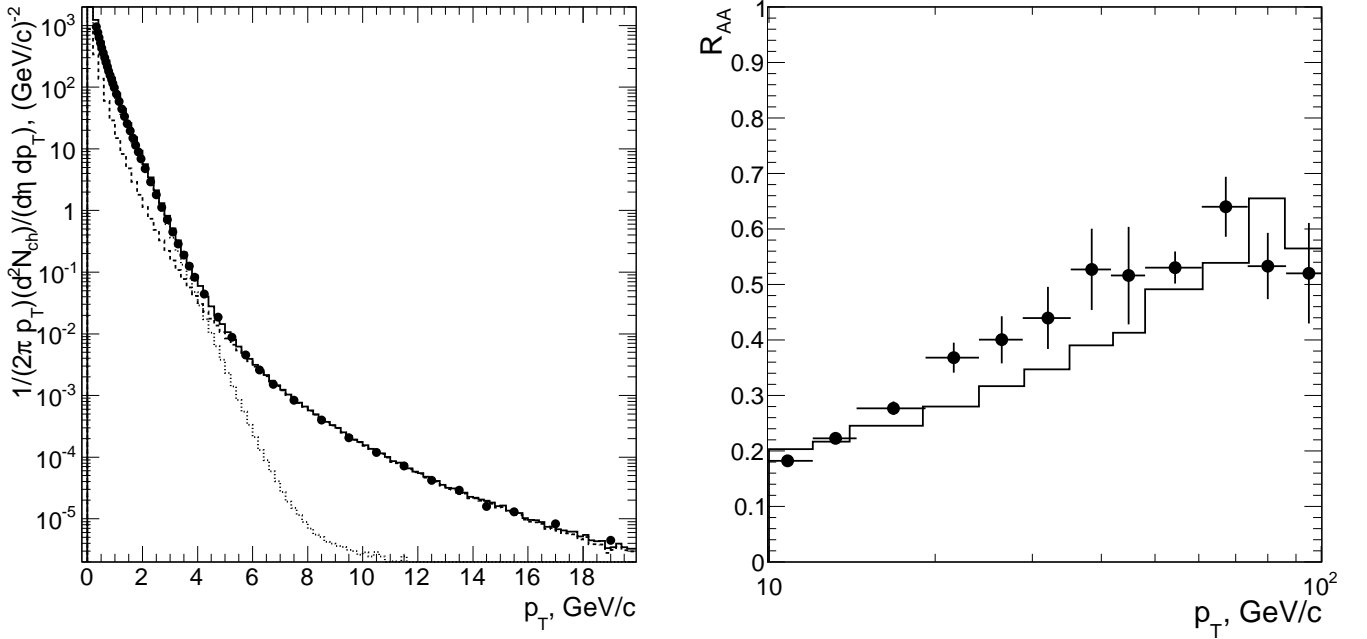


Fig. 2. Charge particle transverse momentum spectrum (left) and nuclear modification factor $R_{AA}(p_T)$ (right) in 5% of most central PbPb collisions at $\sqrt{s_{NN}} = 2.76$ TeV. The points are ALICE [8] (left) and CMS [29] (right) data, histograms are the simulated HYDJET++ events (solid – total result, dashed – hard component, dotted – soft component).

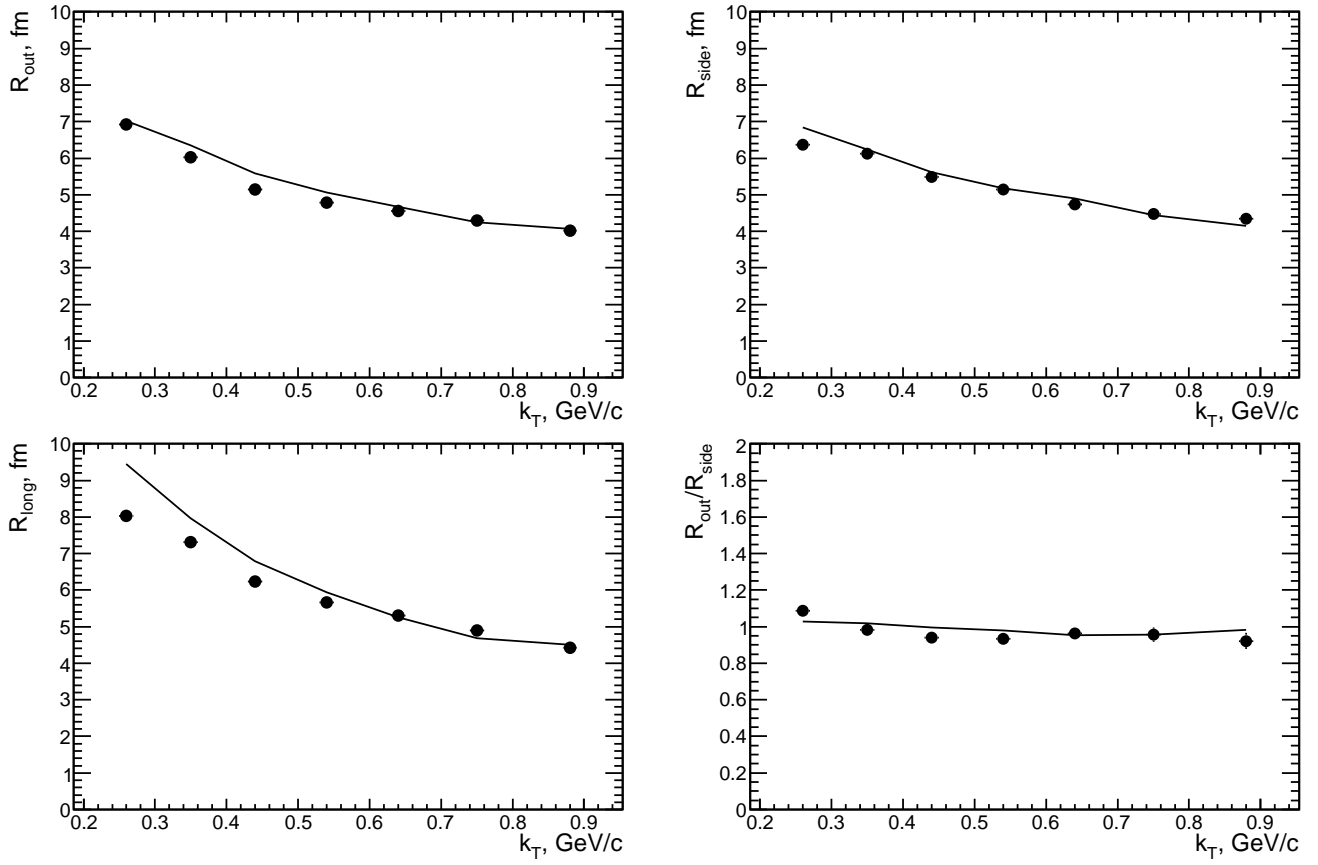


Fig. 3. $\pi^\pm\pi^\pm$ correlation radii as functions of pion pair transverse momentum k_T in 5% of most central PbPb collisions at $\sqrt{s_{NN}} = 2.76$ TeV. The points are the ALICE data [9], curves are the simulated HYDJET++ events.

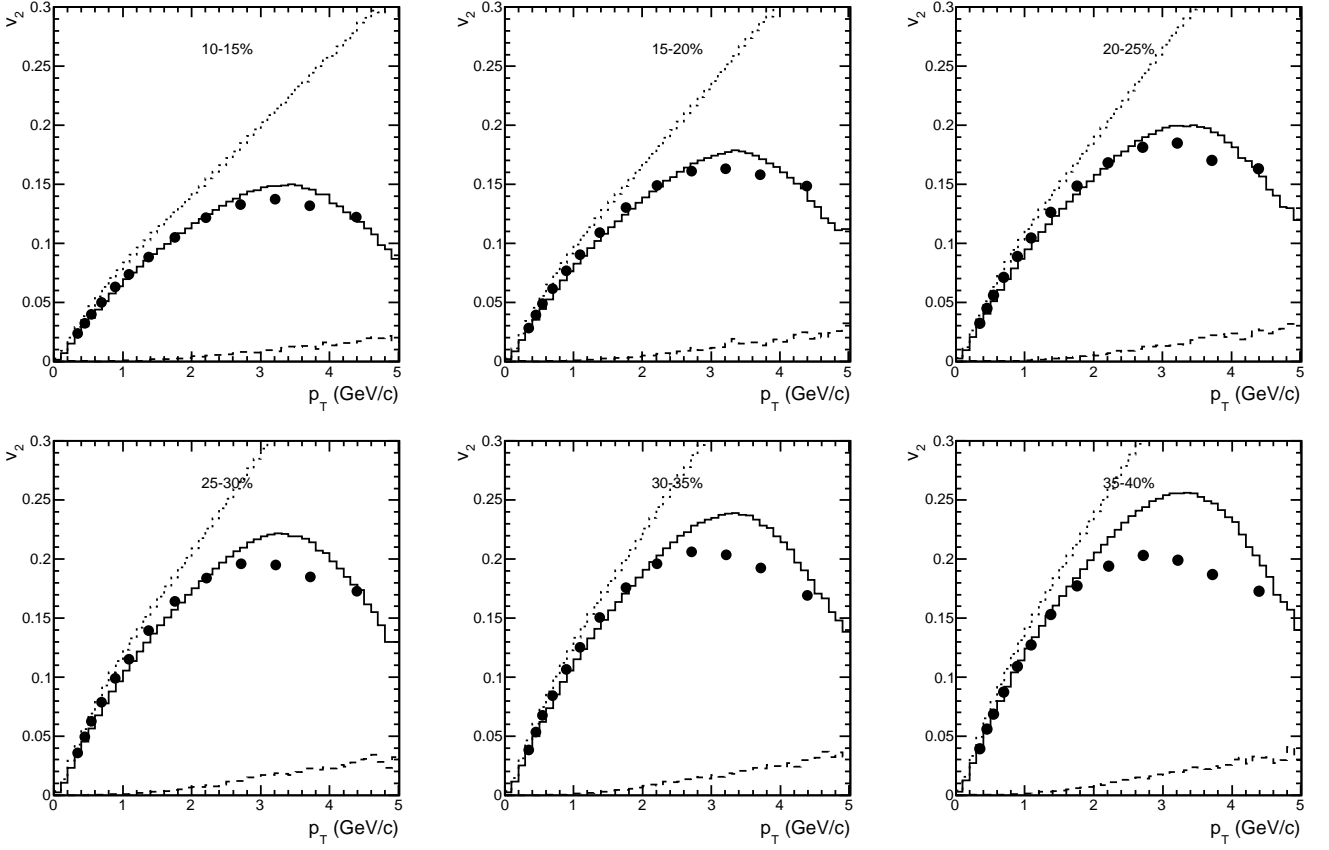


Fig. 4. Elliptic flow coefficient $v_2(p_T)$ for charged hadrons at mid-rapidity ($|\eta| < 0.8$) for different centralities of PbPb collisions at $\sqrt{s_{NN}} = 2.76$ TeV. The points are the CMS data [33], histograms are the simulated HYDJET++ events (solid – total result, dashed – hard component, dotted – soft component).

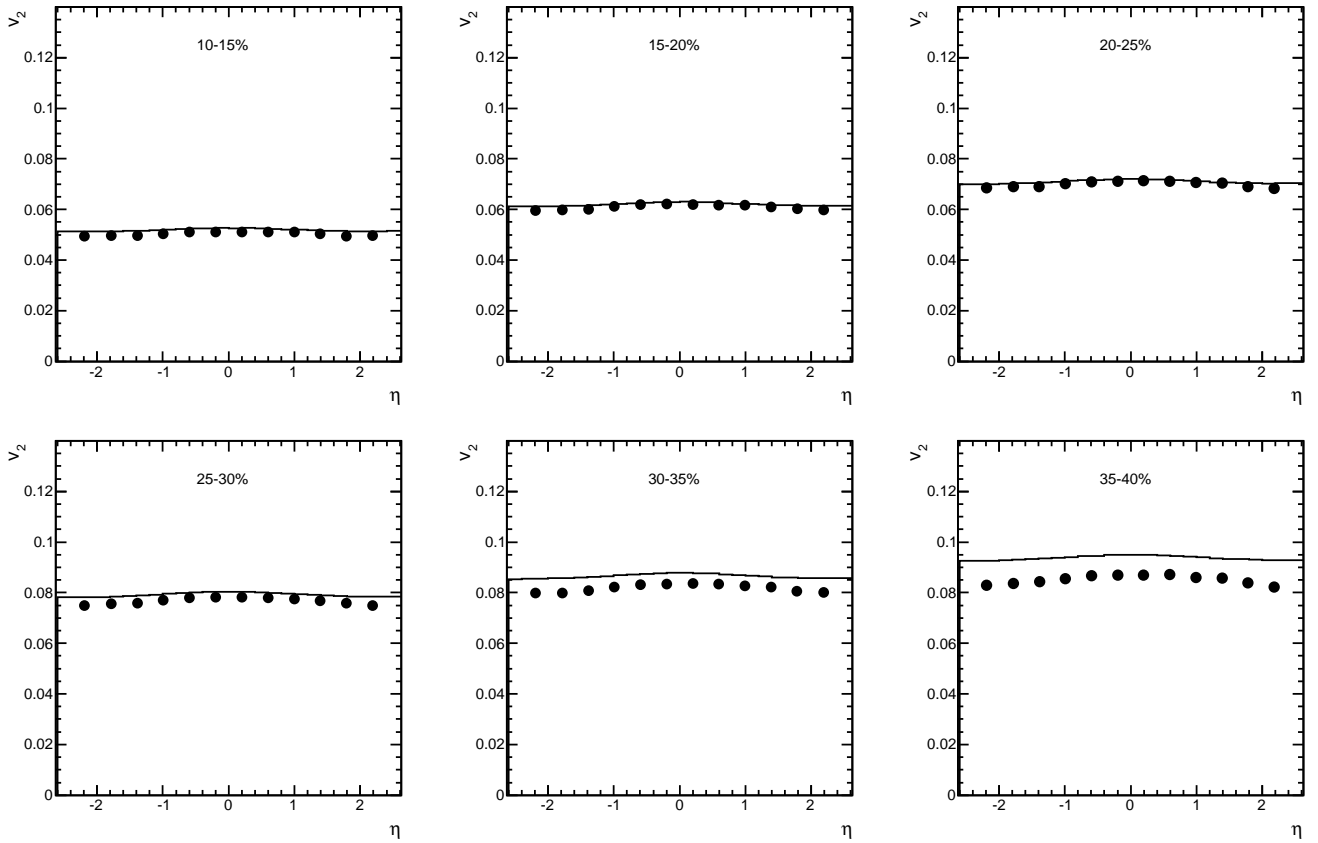


Fig. 5. Elliptic flow coefficient $v_2(\eta)$ ($0.3 < p_T < 3$ GeV/ c) for charged hadrons at different centralities of PbPb collisions at $\sqrt{s_{NN}} = 2.76$ TeV. The points are the CMS data [33], histograms are the simulated HYDJET++ events.